Negative-pion trapping by a metastable state in liquid helium

S. N. Nakamura, M. Iwasaki, H. Outa,* and R. S. Hayano
Department of Physics and Meson Science Laboratory, Faculty of Science, University of Tokyo, Bunkyo-ku, Tokyo 113, Japan

Y. Watanabe,† T. Nagae, and T. Yamazaki
Institute for Nuclear Study, University of Tokyo, Tanashi, Tokyo 188, Japan

H. Tada
Department of Natural Science, College of General Education, University of Tokyo, Komaba, Meguro-ku, Tokyo 153, Japan

T. Numao, Y. Kuno, and R. Kadono†
TRIUMF, Vancouver, British Columbia, Canada V6T 2A3
(Received 6 November 1991)

We have found a long-lived metastable state of stopped π^- in liquid helium by measuring the time spectra of two different delayed products: (i) protons emitted after π^- absorption by ^{4}He nuclei and (ii) 70-MeV electrons originating from free $\pi^- \rightarrow e^- \overline{\nu_e}$ decay. The lifetime and fraction of delayed π^- absorption obtained by using the emitted protons are 7.26 ± 0.12 nsec and $1.66\pm0.05\%$, respectively. The free-decay fraction of a pion in liquid helium was obtained to be $0.64\pm0.03\%$ from this result, which is consistent with the observed free-π^- decay fraction. These results imply that $2.30\pm0.07\%$ of stopped π^- are trapped in the metastable state which have an overall lifetime of 10.1 ± 0.2 nsec. The same experimental and analysis were performed for stopped π^- in liquid neon, where no evidence for trapping was found.

PACS number(s): 36.10.−k

I. INTRODUCTION

Negative mesons stopped in material are normally expected to be absorbed by nuclei immediately ($<10^{-12}$ sec) after mesonic-atom formation. This time is much shorter than the lifetime of such negative mesons as pion and kaon ($\sim10^{-8}$ sec). Thereby, free decay of these particles is not expected to be observed. Recently, however, a slow decay of negative kaons in liquid helium has been observed contrary to this simple picture [1–3]; about 3.5% of stopped K^- in liquid helium decay with a lifetime of about 10 nsec, which is slightly shorter than the lifetime of the free $K^\pm$. This fact indicates that about 4% of stopped K^- in liquid helium are trapped by the metastable state with an overall lifetime of $\sim$60 nsec.

It was already known from helium-bubble-chamber experiments [4–8] that $\sim$2% of stopped K^- and 1% of stopped π^- in liquid helium decay freely. These free decays were interpreted as being due to a hypothetical slow atomic cascade, and the free-decay fraction was simply converted to an average cascade time. The average cascade time thus deduced was in the range of 10^{-10} sec. However, according to the theoretical calculation by Day [9], the cascade time of negative mesons in liquid helium should be less than 10^{-12} sec; the experimental values as deduced above are two orders of magnitude larger than the theoretical calculation. At first, it was believed that there might be unknown mechanisms which could increase the cascade time by two orders of magnitude.

Condo [10] proposed a completely different interpretation, namely, that some fraction of stopped negative mesons in liquid helium are trapped in metastable states and decay freely. In order to determine which interpretation is correct, we have to measure the time spectrum of free decay of negative mesons in liquid helium. If we observe delayed components, this would be a strong evidence for Condo's hypothesis. On the other hand, if we observe only a prompt peak, this will show that the cascade time is long (about 10^{-10} sec) for some unknown reasons. As for K^-, the free-decay components of stopped K^- were found to be 100% delayed [1–3]. Similar trapping states can be expected for π^- and $\bar{p}$ in liquid helium. So, we decided to look for delayed events after π^- stopping in liquid helium. In the meantime, trapping of $\bar{p}$ in liquid helium has been found [11].

II. EXPERIMENTAL SETUP

In order to search for a metastable state, we measured time spectra of delayed products from stopped π^- in liquid helium. There are two ways of observation; one is to observe delayed free decay, and the other is to look for delayed nuclear absorption products. If we observe a lifetime τ_{observe} for delayed fractions of free decay (f_{decay}) and of nuclear absorption (f_{abs}), the lifetime of the trapping state is deduced from

$$1/\tau_{\text{trap}} = 1/\tau_{\text{observe}} - 1/\tau_{\text{free}} , \tag{1}$$

with constraints of

$$f_{\text{decay}} = f_{\text{total}} \frac{\tau_{\text{observe}}}{\tau_{\text{free}}} , \tag{2}$$

$$f_{\text{abs}} = f_{\text{total}} \frac{\tau_{\text{observe}}}{\tau_{\text{trap}}} , \quad (3)$$

$$f_{\text{total}} = f_{\text{decay}} + f_{\text{abs}} . \quad (4)$$

In the case of $\tau_{\text{trap}} > \tau_{\text{free}}$ the decay dominates, while for $\tau_{\text{trap}} < \tau_{\text{free}}$ the absorption dominates. Thus, it is important to measure both channels.

Nearly 100% of pions decay freely to muons, but this muon has a kinetic energy of only 4 MeV, and its range in liquid helium is only a few millimeters. Thus, it is not easy to detect μ^- directly. So, we decided to measure the decay mode of $\pi^- \rightarrow e^- \bar{\nu}_e$. This electron has 70-MeV energy and can escape a liquid target. On the other hand, since this is a rare-decay model (branching ratio equals 1.22×10^{-4}), it is difficult to collect enough statistics with a good signal-to-background ratio. As for nucleus absorption products, we measured protons from π^- absorption by ^{4}He. In this case, a delayed component as well as a prompt component will be revealed in the time spectrum of protons from which the delayed fraction can be obtained directly.

The experiment was carried out at the TRIUMF M13 pion-beam line. The experimental setup is shown in Fig. 1. The incoming pion momentum was 100 MeV/c and its intensity was 5×10^5 π^-/sec. Incoming π^- were stopped in a cylindrical liquid-helium target (23-cm diameter and 31-cm length). They were detected by two scintillation counters (B1 and B2) and a Lucite Čerenkov counter (C_B) located in the beam. The timing and pulse-height information from these counters were used for particle identification. Beam particles which passed through the target were detected by a large veto counter (A1). The energy spectra of outgoing electrons and protons from stopped pions were measured by a large NaI(Tl) spectrometer (TINA) of 46-cm diameter and 51-cm length. It was used at TRIUMF for the precise determination of the branching ratio of $\pi^+ \rightarrow e^+ \nu_e$ process [12]. It was located at 90° with respect to the beam. For particle identification and timing measurements of outgoing particles, two scintillation counters (T1 and T2) and one Lucite Čerenkov counter (C_T) were placed in front of TINA.

The tracks of incoming and outgoing particles were measured to reconstruct the stopping position of a π^- in the target using beam-line multiwire proportional chambers (MWPC) (BC1, BC2) and telescope MWPC's (PC1–PC4). This information was used not only for fiducial cuts but also for calculating the flight time of π^- until stopping [T(B1-stop)] and the flight time of the outgoing particle from the vertex to the T1 counter [T(stop-T1)]. We can calculate T(B1-stop) from the pion range, T(stop-T1) from the π^- stopping position, and the energy of the outgoing particle measured by TINA.

We can obtain a trapping time of π^- (T_{trap}) for each event as follows:

$$T_{\text{trap}} = T(\text{B1-T1}) - T(\text{B1-stop}) - T(\text{stop-T1}) ,$$

where T(B1-T1) is a time difference between the B1 hit and T1 hit. The time spectrum of T(B1-T1) was measured by using a LeCroy 2228 time-to-digit converter (TDC) in the range from −50 to 200 nsec.

The trigger condition necessary for data acquisition was as follows:

$$\text{trigger} = \text{B1} \cdot \text{B2} \cdot \overline{\text{A1}} \cdot \text{T1} \cdot \text{T2} \cdot \overline{\text{computer veto}} .$$

All data were acquired by a PDP-11–compatible computer-automated measurement-and-control (CAMAC) module (CES-J11). A CAMAC-VAX interface (K3922-K2922) transferred the data obtained by CES-J11

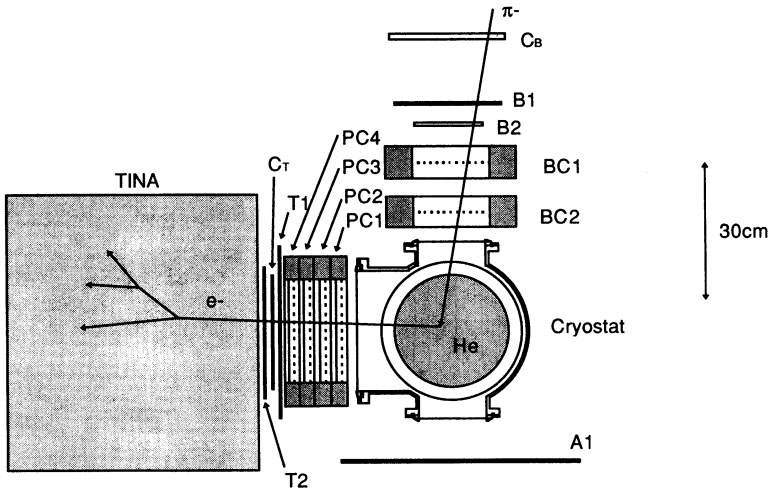

FIG. 1. A schematic figure of the experiment setup. TINA labels a large NaI(Tl) spectrometer; BC and PC denote MWPC's; C denotes Lucite Čerenkov counter; B and T denote scintillation counters; and A1 is a veto counter.

to a VAX station II. They were recorded on an 8-mm VCR tape. The typical event rate was about 280 events/sec.

Data were also taken with π^+ beam in the same conditions, which provided a sample of *capture-free* decays. Positrons from free decay ($\pi^+ \rightarrow e^+ \nu_e$) were used to normalize the acceptance for electrons from $\pi^- \rightarrow e^- \bar{\nu}_e$, including the solid angle and the off-line analysis efficiencies. At the same time, we can calibrate the energy scale of TINA using the 70-MeV monochromatic positrons.

The data were taken for 200 h of π^- and for 10 h of π^+. In addition, a similar measurement for liquid neon was performed for 30 h.

III. DATA ANALYSIS

A. Incoming π^- identification

The incoming beam is synchronized with the rf timing of the cyclotron. Therefore, the rf timing represents the time when the secondary particles are created at the production target. The time between the rf timing and the particle arrival at the B1 counter corresponds to the time of flight (TOF) of the particles.

The velocities of 100 MeV/c π^+ and μ^- are 0.58 and 0.67 of the speed of light, respectively. The distance between the production target and the B1 counter was about 10 m. Hence, the difference of TOF between π^- and μ^- was about 8 nsec. They are easily separated in an off-line analysis. Figure 2 shows the TOF difference and pulse height of the B1 counter. When two particles come in the same rf packet, the pulse height would be doubled. Thus, pileup events were rejected even when two particles belong to the same rf packet. The central part enclosed by the lines was chosen to reject μ^-, e^- and multi-π^- events. This procedure reduced the μ^- contamination to be less than 0.11%.

B. Outgoing particle selection

The energy deposit in the T1 counter was used to distinguish electrons from protons. The top figure of Fig. 3 shows the energy distribution in the T1 counter. Protons and electrons are well separated. The bottom figure of Fig. 3 shows similar distribution for the events which had energy greater than 50 MeV. As seen in Fig. 3 (bottom), e^+e^- pairs created by high-energy γ rays originating from the radiative π^--capture process ($\pi^- + \mathrm{He} \rightarrow \gamma + X$; branching ratio 1.5%) are also observed. They formed the background in the high-energy region for the observation of 70-MeV electrons. We excluded events in this region.

C. Determination of the π^- stopping point

We had two MWPC's (BC1, BC2) to determine the track of an incoming pion. In addition, we had four MWPC's (PC1~PC4) to determine the track on an outgoing particle, which was obtained by the least-squares fitting of positions in the MWPC's.

Events which had vertices more than 35 mm from the wall of the target were accepted. The vertex resolution is better than 20 min (rms) for outgoing e^-. Use of this fiducial cut rejected more than 90% of the events arising from interactions in the wall.

D. Energy-loss correction

The charged particles which passed through the target material lose energy. A correction has to be applied to the energy measured by TINA to get the original energy. We corrected their energy deposit in material using vertex information from MWPC's.

E. Pileup rejection

In order to obtain a genuine time spectrum in our time window (200 nsec) we have to correct for pre- and post-pileup events which would distort the time spectrum. If another pion comes into the target within the time win-

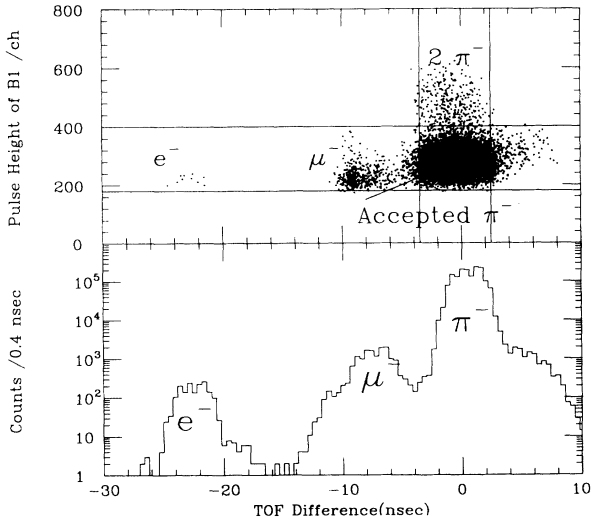

FIG. 2. TOF difference vs pulse height of the B1 counter (top) and TOF distribution (bottom).

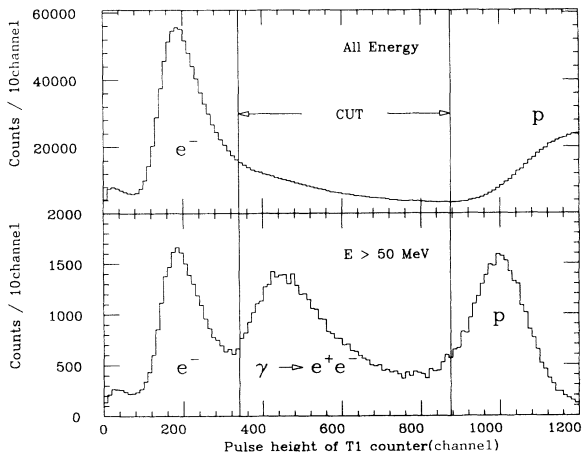

FIG. 3. Energy-deposit distribution in the T1 counter (top), and the same figure with $E > 50$ MeV selection (bottom).

dow, we cannot identify which pion produced the outgoing particle. This is avoided by discarding any event which had additional hits within a time range of 1 μsec before or 200 nsec after a pion struck the B1 counter. The same pileup rejection was done for the outgoing particles as well.

A similar pileup rejection was applied to the TINA energy spectrum to minimize the energy shift caused by pileup hits. The output signal of TINA was integrated in three different time ranges (TINA-early, TINA-normal, TINA-late). TINA-normal refers to the signal with a normal timing gate, while TINA-early's gate started 200 nsec before the triggered event, and TINA-late's gate started 200 nsec after the event. We rejected pre-pileup of TINA, eliminating the events which had a signal in the TINA-early spectrum. Similarly, we discarded post-pileup of TINA by removing the events when a linear relation between TINA-normal and TINA-late was lost.

IV. RESULTS FOR HELIUM DATA

A. Proton time spectrum

Figure 4 shows a trapping-time spectrum of emitted protons which came from π^- absorption by ^{4}He. There is a delayed component as well as a prompt peak. The delayed component looks like a single exponential function within present experimental accuracy. This time spectrum was fitted to a function

$$N(t)=A\exp\left[-\frac{t}{\tau}\right]+B\exp\left[-\left[\frac{t}{\Gamma}\right]^2\right]+C$$

$$(A=0 \text{ when } t<0),$$

where τ and Γ are the lifetime of delayed events and the width of the prompt peak, respectively.

The observed lifetime of the delayed component was $\tau_{\text{observe}}=7.26\pm0.12$ nsec. Using Eq. (1) with $\tau_{\text{free}}=26.03$ nsec we obtain $\tau_{\text{trap}}=10.06\pm0.22$ nsec. The ratio of the delayed events to the prompt gives $f_{\text{abs}}=1.66\pm0.05\%$, where the error is purely statistical.

If an in-flight reaction occurs, the number of prompt events may involve ambiguity. Using Monte Carlo simulation, the prompt fraction caused by the in-flight reactions was estimated to be less than 0.01%, which we can safely neglect.

Using these values in Eqs. (2) and (3), we obtained the free-decay fraction

$$f_{\text{decay}}=(1.66\pm0.05\%)\frac{10.06\pm0.22 \text{ nsec}}{26.03 \text{ nsec}}$$

$$=0.64\pm0.03\% .$$

This value can be compared with the result obtained from the 70-MeV electrons from $\pi^-\rightarrow e^-\bar{\nu}_e$ decay. The total trapped fraction (f_{total}) of π^- in liquid helium is given by the sum of f_{abs} and f_{decay}. It is $2.30\pm0.07\%$ of stopped π^- in liquid helium.

B. 70-MeV electron time spectrum

Figure 5 shows an energy spectrum for the delayed electrons ($2<T_{\text{trap}}<10$ nsec). There is a peak at 70 MeV from the $\pi^-\rightarrow e^-\bar{\nu}_e$ free decay. Figure 6 is a time spectrum of the events in this energy region ($60<E<80$ MeV). A sharp prompt peak originates from the radiative pion-capture process followed by the pair creation [$\text{He}(\pi^-,\gamma),\gamma\rightarrow e^+e^-$]. The peak at $t=-8.5$ nsec comes from μ^- scattering (μ^- arrived at 8.5 nsec earlier than π^-). This time spectrum was fitted to the following function:

$$N(t)=A\exp\left[-\frac{t}{\tau}\right]+B\exp\left[-\left[\frac{t}{\Gamma}\right]^2\right]$$

$$+C\exp\left[-\left[\frac{t-t_\mu}{\Gamma_\mu}\right]^2\right]+D$$

$$(A=0 \text{ when } t<0).$$

This function is similar to that of protons, except for the μ^- component. The observed lifetime of the delayed component was $\tau_{\text{observe}}=7.2\pm1.4$ nsec. The free-decay fraction (f_{decay}) was obtained as follows by comparing with the π^+ data, where 100% of stopped π^+ in material

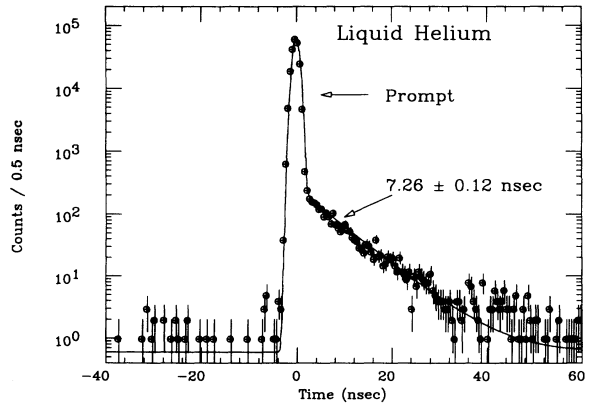

FIG. 4. A time spectrum of protons from stopped π^- in liquid helium.

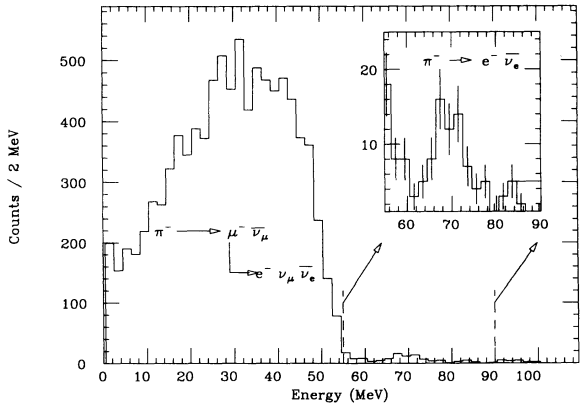

FIG. 5. An energy spectrum of e^- from stopped π^- in liquid helium ($2<T_{\text{trap}}<10$ nsec).

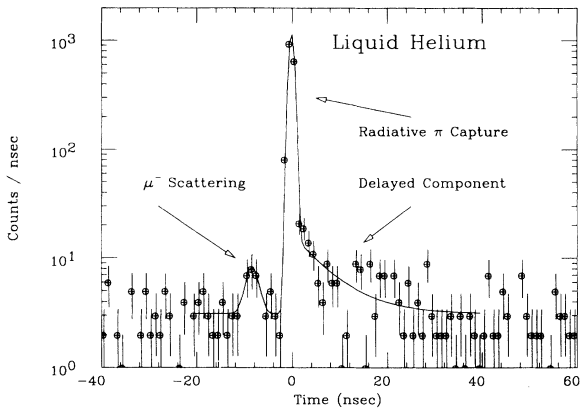

FIG. 6. A time spectrum of e^- in the region 60 MeV $< E <$ 80 MeV from stopped π^- in liquid helium.

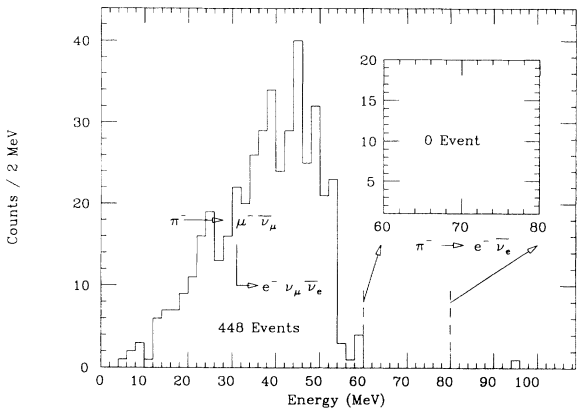

FIG. 8. An energy spectrum of e^- from stopped π^- in liquid neon ($2 < T_{\text{trap}} < 30$ nsec).

are free from nuclear absorption:

$$f_{\text{decay}} = \frac{N_{70\text{-MeV } e^-}/N_{\text{stopped } \pi^-}}{N_{70\text{-MeV } e^+}/N_{\text{stopped } \pi^+}} ,$$

where $N_{70\text{-MeV } e^\pm}$ and $N_{\text{stopped } \pi^\pm}$ are the numbers of $e^\pm$ from free decay and of stopped $\pi^\pm$ in the target, respectively. The free-decay fraction of stopped π^- in liquid helium was obtained as $f_{\text{decay}} = 0.93 \pm 0.35\%$. A rather large error was caused by low statistics and large background from the radiative π^--capture process. This result is consistent with the result obtained from the emitted protons.

V. RESULTS FOR NEON DATA

The same analysis was performed on data from stopped π^- in liquid neon. Figure 7 is a trapping-time spectrum obtained by emitted protons. In this time spectrum, we observe no delayed component. (One event at $t \sim 20$ nsec is consistent with background level.) Figure 8 shows an energy spectrum of delayed electrons, where we observe no 70-MeV electrons which would be indicative of trapping.

We obtain an upper limit of the free-decay fraction (f_{decay}) of π^- in liquid neon. The π^+ data were used for normalization. This result can be translated into an upper limit of the trapping fraction (f_{total}) using Eq. (2).

As for proton data, we can obtain an even more stringent upper limit for the trapping fraction by substituting the number of observed prompt events (2.9×10^4) for N_{prompt} in the following equations (the factor of 2.3 is inserted to assure a 90% confidence level in Poisson distribution):

$$f_{\text{total}} < 2.3 \frac{A}{B} \frac{\tau_{\text{trap}}}{\tau_{\text{observe}}} ,$$

where

$$A = \tau_{\text{observe}} \left[\int_4^{40} \exp\left(-\frac{t}{\tau_{\text{observe}}} \right) dt \right]^{-1} ,$$

$$B = N_{\text{prompt}} - \frac{A}{\tau_{\text{observe}}} \int_0^4 \exp\left(-\frac{t}{\tau_{\text{observe}}} \right) dt ,$$

and

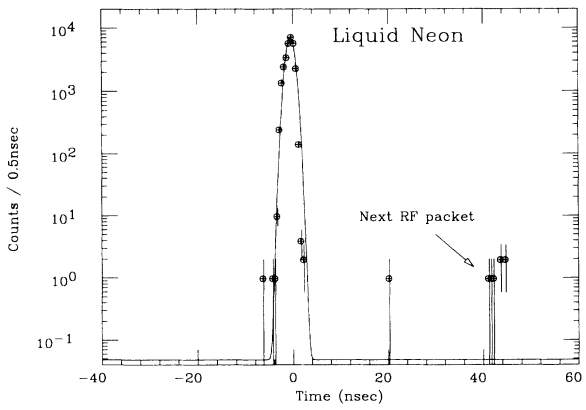

FIG. 7. A time spectrum of protons from stopped π^- in liquid neon.

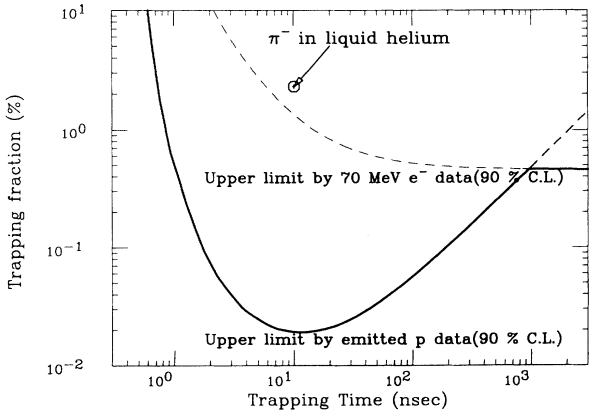

FIG. 9. Upper limit of a π^- trapping fraction in liquid neon as a function of trapping time.

$$(\tau_{\text{observe}})^{-1}=(\tau_{\text{trap}})^{-1}+(\tau_{\text{free}})^{-1} .$$

Figure 9 shows an upper limit of the π^- trapping fraction with a 90% confidence level in liquid neon as a function of the lifetime of the metastable state (τ_{trap}).

VI. DISCUSSIONS

We have observed delayed nuclear absorption and free decay of π^- in liquid helium. The present result demonstrates that the trapping hypothesis is correct not only for K^- and $\bar{p}$ but also for π^-. Condo [10] asserted that the (π^--e^--α) system accommodates metastable states when a π^- ejects one electron from a helium atom and occupies a circular orbital of large n. This idea was extended theoretically by Russell who calculated the lifetime of a (X^--e^--α) system where X^- is a negative hadron (K^-, π^-, or $\bar{p}$) [13]. For the antiproton, more recent calculations by Ahlrichs *et al.* [14] and by Yamazaki and Ohtsuki [15] are available.

Experimental data on trapping states of negative hadrons in liquid helium are summarized in Fig. 10 (π^- (present work); K^- [1–3]; $\bar{p}$ [11]).

The antiproton data could not be fitted by a single exponential function, so Iwasaki *et al.* [11] fitted it by assuming four delayed components. The present π^- data show a single exponential decay. The dashed lines in Fig. 10 represent the lifetimes of free negative hadrons. The present observation that the trapping lifetime of π^- is shorter than those of K^- and $\bar{p}$ is consistent with the Condo-Russell scenario, where a proportionality of the trapping lifetime to the square of the reduced mass is expected [15].

The Condo-Russell scenario can explain a tendency for the lifetime to increase as the negative hadron becomes heavier. However, it cannot quantitatively account for the time distribution shape, lifetime, or trapping fraction. Complete understanding of these trapping phenomena will require detailed knowledge concerning the formation of metastable states and their collisional excitation and deexcitation. The trapping time strongly depends on the initial state into which the negative hadron is captured. It is also important to examine whether the same phenomena occur when the physical conditions (density, temperature, etc.) are changed. In particular, it is important to stop negative hadrons in less dense media where the atomic distance is large. From this viewpoint, experiments with antiprotons are very attractive, because antiprotons are stable particles and there is no limitation on the observable time window. Furthermore, antiprotons are available as a low-energy beam and can be stopped in gas. Extensive experiments on various phases of gaseous helium are being planned.

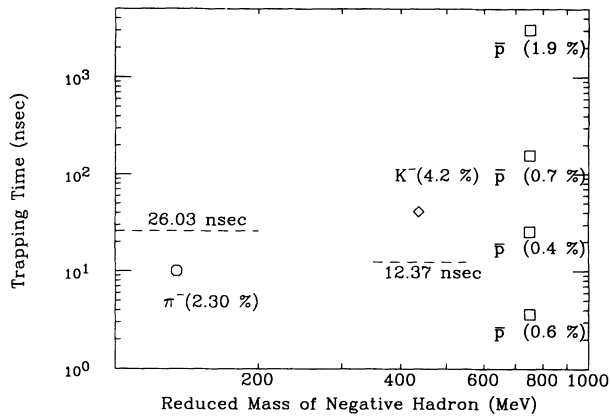

FIG. 10. The observed trapping times of negative hadrons in liquid helium vs the reduced mass of a negative hadronic helium atom. The dashed lines represent the lifetime of free negative hadrons.

ACKNOWLEDGMENTS

The authors are pleased to acknowledge Dr. E. Widmann, Dr. H. Tamura, and Dr. E. Takada for their helpful suggestions and discussions. We are grateful to the TRIUMF cryogenic staff for their support to this experiment. We used the VAX-based computer system of UTMSL for data analysis. Two of the authors (S.N.N. and H.O.) received support from Japan Society for the Promotion of Science. This work was supported in part by the Grant-in-Aid on International Science Research of the Japanese Ministry of Education, Culture and Science.

*Present address: Institute for Nuclear Study, University of Tokyo, Tanashi, Tokyo 188, Japan.
†Present address: Institute of Physical and Chemical Research (RIKEN), Wako, Saitama 351-01, Japan.

[1] T. Yamazaki, M. Aoki, M. Iwasaki, R. S. Hayono, T. Ishikawa, H. Outa, E. Takada, H. Tamura and A. Sakaguchi, Phys. Rev. Lett. **63**, 1590 (1989).
[2] R. S. Hayano, in *Electromagnetic Cascade and Chemistry of Exotic Atoms,* edited by L. M. Simons *et al.,* Ettore Majorana International Science Series 52 (Plenum, New York, 1990), p. 141.
[3] H. Outa, (unpublished).
[4] J. G. Fetkovich and E. G. Pewitt, Phys. Rev. Lett. **11**, 290 (1963).
[5] M. M. Block, T. Kikuchi, D. Koetke, J. Kopelman, C. R. Sun, R. Walker, G. Culligan, V. L. Telegdi, and R. Winston, Phys. Rev. Lett. **11**, 301 (1963).
[6] M. M. Block, J. B. Kopelman, and C. R. Sun, Phys. Rev. **140**, 143 (1965).
[7] J. G. Fetkovich, J. McKenzie, B. R. Riley, I.-T. Wang, K. Bunnell, M. Detrick, T. Fields, L. G. Hyman, and G. Keyes, Phys. Rev. D **2**, 1803 (1970).
[8] C. Comber, D. H. Davis, J. Gordon, D. N. Tovee, R. Roosen, C. Vander Velde-Wilquet, and J. H. Wickens, Nuovo Cimento A **24**, 294 (1974).
[9] T. B. Day, Nuovo Cimento **18**, 381 (1969).

[10] G. T. Condo, Phys. Lett. **9**, 65 (1964).
[11] M. Iwasaki, S. N. Nakamura, K. Shigaki, Y. Shimizu, H. Tamura, T. Ishikawa, R. S. Hayano, E. Takada, E. Widmann, H. Outa, M. Aoki, P. Kitching, and T. Yamazaki, Phys. Rev. Lett. **67**, 1246 (1991).
[12] D. A. Bryman, R. Dubois, J. A. Macdonald, T. Numao, B. Olaniyi, A. Olin, J. M. Poutissou, and M. S. Dixit, Phys. Rev. D **33**, 1211 (1986).
[13] J. E. Russell, Phys. Rev. Lett. **23**, 63 (1969); Phys. Rev. A **1**, 721 (1970); **1**, 735 (1970); **1**, 742 (1970).
[14] R. Ahlrichs, O. Dumbrajs, H. Pilkuhn, and H., G. Schlaile, Z. Phys. A **306**, 297 (1982).
[15] T. Yamazaki and K. Ohtsuki, Phys. Rev. A (to be published).

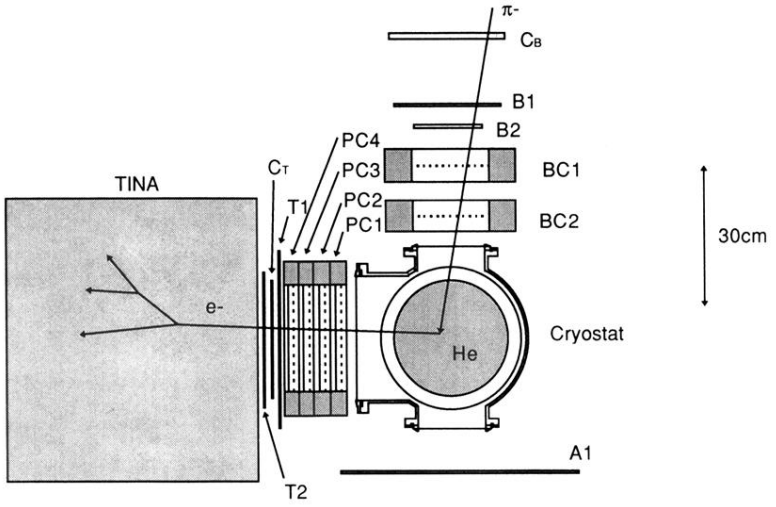

FIG. 1. A schematic figure of the experiment setup. TINA labels a large NaI(Tl) spectrometer; BC and PC denote MWPC's; C denotes Lucite Čerenkov counter; B and T denote scintillation counters; and A1 is a veto counter.